

# On the Importance of the Purely Gravitationally Induced Density, Pressure, and Temperature Variations in Gravity Waves: Their Application to Airglow Observations

U. MAKHLOUF

*Physics Department, University of Cincinnati, Cincinnati, Ohio*

E. DEWAN

*Optical Physics Division, Air Force Geophysics Laboratory, Hanscom Air Force Base, Bedford, Massachusetts*

J. R. ISLER AND T. F. TUAN

*Physics Department, University of Cincinnati, Cincinnati, Ohio*

A quantitative study is made of the relative importance of the purely gravitationally induced compression (GIC) due to fluid particle altitude change and the actual "wave compression" which can occur at a fixed altitude in a gravity wave. The results for density, pressure, and temperature variations show the following: (1) the GIC effects predominate (>95%) for  $v/c < 20\%$ , where  $v$  is the horizontal phase velocity and where very simple formulas can be obtained; (2) the relative importance depends strongly on frequency for wave periods less than 10 min but becomes totally independent of frequency for periods greater than 20 min; and (3) the temperature measurements can be quickly converted to height variations wherever the GIC effect predominates; in general, the conversion is equivalent to the adiabatic lapse rate, i.e., a  $10^\circ$  temperature variation corresponds to a height change of 1 km. In addition, the total kinetic energy density can be simply expressed in terms of height variation and, whenever the GIC effects predominate, can be very easily obtained from temperature measurements. An interesting by-product has been that for waves of small horizontal phase speed, the total wave kinetic energy at any frequency is equal to the kinetic energy of the natural (Brunt) oscillation of an air parcel with the same vertical displacement.

## 1. INTRODUCTION

The purpose of the present paper is to determine the degree to which gravity waves (to be abbreviated GW) are subject to purely gravitationally induced expansions and compressions (GIC) from altitude changes of a given parcel of air and the degree to which they are caused by purely "wave compression." (By purely "wave compression" we mean the acoustic component of the gravity waves.) If for certain types of GW the GIC effects can cause most (say 90%) of the GW variations so that we can neglect "wave compression," then the resulting simplification [Dewan *et al.*, 1988] can allow us to use very simple formulas for the GW parameters (density, pressure, and temperature fluctuations) as well as to make quick estimates of other GW parameters. For instance, a quick conversion from temperature fluctuations to height fluctuations can be readily effected, and the latter can be used for a quick estimate of the kinetic energy density. This is also very useful in airglow measurements where interferometer measurements give temperature directly and hence airglow height changes can be estimated.

We will begin by showing that the density, pressure, and temperature fluctuations can be explicitly expressed as a sum of two terms: one describing the GIC compression, and the other the "wave motion." The former vanishes in the

absence of gravity ( $g = 0$ ), while the latter remains in altered form and provides for purely longitudinal acoustic wave compression.

For  $g \neq 0$ , the relative importance of these two effects depends on the magnitude of the horizontal phase velocity of the GW as compared to the speed of sound. For small-scale GW, where by definition we mean the phase velocity is much less than the speed of sound and the wavelength is also small, we have found that indeed the GIC effects predominate. Since many of the observed mid-latitude airglow fluctuations (including OH) involve relatively small scale GW [Witt, 1962; Clairemidi *et al.*, 1985; Taylor and Hapgood, 1988] with low horizontal phase velocity  $v < 70 \text{ m s}^{-1}$  [Vincent and Reid, 1983], we may, for most cases, assume that the density, pressure, and temperature variations are GIC and a quick conversion to height variations may be made. Very simple formulas for the kinetic energy density can be derived, where  $k_z^2 > 0$ , both for the general case and even more so in the GIC approximation.

We should point out that there is considerable interference between the two effects and that only if either is greater in magnitude than the other by a large factor can we comfortably neglect the smaller terms. To test the limits of this criterion, we will consider three specific experimental observations: the first being the airglow observation made by Taylor and Hapgood [1988] (in association with the MAP-STAR program) which easily meets our criterion; the second being the wave observations by Clairemidi *et al.* [1985] which also meet our criterion; and the third being the

Copyright 1990 by the American Geophysical Union.

Paper number 89JA02812.  
0148-0227/90/89JA-02812\$05.00

AD-A231 833

DISSEMINATION  
Approved  
Distribution

DTIC  
ELECTE  
JAN 09 1991  
S B D

observations on noctilucent clouds made by Witt [1962] which is marginally above the limits of our criterion. The results show that for all three sets of observations the simple GIC model is surprisingly accurate and that one may safely assume that many of the mid-altitude density, pressure, and temperature fluctuations are governed by GICs. In general, we have proved that in the region  $v \ll C$  where the GIC expansion or contraction effects dominate, a 10°K variation in temperature would indicate an altitude change of 1 km of a parcel of air. We have also found that in the same region the kinetic energy density is equivalent to that of the free vertical oscillation of an air parcel with the same vertically displaced amplitude and is independent of the wave frequency. Thus the above conversion can be immediately used to calculate the kinetic energy density.

## 2. GIC EXPANSION AND CONTRACTION

When a fluid element is displaced by a vertical distance  $h$  in a hydrostatic fluid, its density is compressed by an amount  $\Delta\rho_a$ . This density change  $\Delta\rho_a$  is produced by a change in background pressure,  $\Delta p$  (where  $\Delta p = (\partial p_0/\partial z)h = c^2\Delta\rho_s$  and  $\Delta\rho_s$  is the density variation due purely to adiabatic compression), minus the change in background density,  $\Delta\rho_0 = (\partial\rho_0/\partial z)h$ . One can show that in a uniform isothermal background atmosphere with scale height  $H$ ,

$$\frac{\Delta\rho_a}{\rho_0} = \frac{\Delta\rho_s}{\rho_0} - \frac{\Delta\rho_0}{\rho_0} = \left(\frac{\gamma-1}{\gamma}\right) \frac{h}{H} \quad (1)$$

where we have used the fact that  $c^2\rho_0 = \gamma p_0$  and

$$\frac{1}{\rho_0} \frac{\partial\rho_0}{\partial z} = -H^{-1} = \frac{1}{p_0} \frac{\partial p_0}{\partial z}$$

## 3. A COMPARISON OF THE GIC AND WAVE COMPRESSION

In a GW with frequency  $\omega$ ,  $h = w/i\omega$  (to first order) where  $h$  and  $w$  are the vertical displacement and velocity fields, respectively. At the Brunt frequency,  $\omega = \omega_b$ , the atmosphere would just oscillate vertically at its natural frequency with the density fluctuations given by (1). In general, by using Hines' [1960] formula for  $\Delta p/\rho_0$ ,  $h = w/i\omega$ , and horizontal velocity field  $u$  we can show that to the first order (see Appendix 1),

$$\frac{\Delta\rho}{\rho_0} = \left(\frac{\gamma-1}{\gamma}\right) \frac{h}{H} + \left(\frac{v}{c}\right)^2 \left(\frac{u}{v}\right) = \frac{\Delta\rho_a}{\rho_0} + \frac{\Delta\rho_c}{\rho_0} \quad (2a)$$

where  $u$  is the horizontal particle velocity,  $v (=v_x)$  is the horizontal phase velocity, and  $\Delta\rho_c/\rho_0 (=v/c)^2 (u/v)$  is the density fluctuation due to wave compression. From (2a) it is clear that  $\Delta\rho_a/\rho_0 \rightarrow 0$  as  $g \rightarrow 0$  since  $H = c^2/\gamma g$ , and the terms  $\Delta\rho_c/\rho_0$  will be appropriately changed to provide for the purely longitudinal wave compression at all frequencies for sound wave propagation in the absence of gravity. As  $g \rightarrow 0$ ,  $H \rightarrow \infty$ , and using (A22) we obtain

$$\frac{|\Delta\rho|}{\rho_0} \xrightarrow{g \rightarrow 0} \frac{|\Delta\rho_c|}{\rho_0} = \frac{|uv|}{c^2} = \frac{(|u|^2 + |w|^2)^{1/2}}{c} \quad (2b)$$

and

$$\frac{|u|}{|w|} \xrightarrow{g \rightarrow 0} \frac{k_x}{k_z}$$

where  $k_x$  is the horizontal wave vector. Equation (2b) clearly shows a purely longitudinal wave compression when  $g = 0$ . From now on we shall only be concerned with  $g \neq 0$ . In that case, from (2a) the relative importance of  $\Delta\rho_a/\rho_0$  and  $\Delta\rho_c/\rho_0$  depends on  $(v/c)$  and, in order to remain well below the Lindzen [1981] limit for GW saturation,  $|u| < v$  [see Fritts, 1984]. Clearly, for small-scale GW where  $v \ll C$ , the density variation comes mainly from GIC compression,  $\Delta\rho_a/\rho_0$ . On the other hand, for  $v \rightarrow C$  and close to the limit for GW saturation the wave compression  $\Delta\rho_c/\rho_0$  is large, and we need to include both effects.

In general, since both  $\Delta\rho_a/\rho_0$  and  $\Delta\rho_c/\rho_0$  are complex quantities with different phases, considerable interference occurs between the two terms, and only if one has a magnitude of at least 4–5 times greater than the other can we neglect the other term.

To make a quantitative comparison between  $\Delta\rho_a$  and  $\Delta\rho_c$ , we plot  $|\Delta\rho_a|/|\Delta\rho|$  and  $|\Delta\rho_c|/|\Delta\rho|$  as a function of  $v/c$ . It can be shown for  $k_z^2 > 0$  (see Appendix 2) that

$$\frac{|\Delta\rho_a|}{|\Delta\rho|} = \left[ \frac{(\gamma-1)\{1-(v/c)^2\}}{(\gamma-1) - (\omega/\omega_b)^2(v/c)^2} \right]^{1/2} \quad (3)$$

$$\frac{|\Delta\rho_c|}{|\Delta\rho|} = \left[ \frac{1 - (\omega/\omega_b)^2}{(\gamma-1) - (\omega/\omega_b)^2(v/c)^2} \right]^{1/2} \left(\frac{v}{c}\right) \quad (4)$$

Thus, in general,  $|\Delta\rho_a|/|\Delta\rho|$  begins with the value unity (i.e., density variations are due entirely to GIC compression) at  $v/c = 0$ , while  $|\Delta\rho_c|/|\Delta\rho|$  begins at zero (i.e., no wave compression). As can be seen from (3) and (4), when  $v/c$  increases, the behavior of  $|\Delta\rho_a|/|\Delta\rho|$  and  $|\Delta\rho_c|/|\Delta\rho|$  depends entirely on  $\omega/\omega_b$  for any value of  $v/c$ .

For long-period gravity waves where  $\omega \ll \omega_b$ , we may neglect the terms involving  $\omega/\omega_b$  in the denominator for both  $|\Delta\rho_a|/|\Delta\rho|$  and  $|\Delta\rho_c|/|\Delta\rho|$ . For such cases,

$$\frac{|\Delta\rho_a|}{|\Delta\rho|} \sim \left[ 1 - \left(\frac{v}{c}\right)^2 \right]^{1/2} \quad (5)$$

$$\frac{|\Delta\rho_c|}{|\Delta\rho|} \sim \left(\frac{1}{\gamma-1}\right)^{1/2} \left(\frac{v}{c}\right) \quad (6)$$

and  $|\Delta\rho_a|/|\Delta\rho|$  drops from unity as  $v/c$  increases while  $|\Delta\rho_c|/|\Delta\rho|$  increases linearly with  $v/c$ .

Figure 1 shows this behavior for gravity waves with periods greater than 20 min. Actually, there is little variation with period from 20 min on up, and a plot at  $\tau = 120$  min falls exactly on top of the corresponding curves at 20 min. Both curves are plotted from (3) and (4), but there would have been no difference if we had used (5) and (6). At  $\tau = 10$  min (Figure 2),  $|\Delta\rho_c|/|\Delta\rho|$  begins to deviate from a straight line but only slightly.  $|\Delta\rho_a|/|\Delta\rho|$  drops somewhat less as  $v/c$  increases, showing an increase in importance relative to wave compression for a given phase velocity. Furthermore, the crossover between the GIC compression and the wave compression remains fairly constant at  $v/c \sim 55$ –60%. In general, for GW with frequencies in this range (i.e.,  $\tau > 10$  min), if we use the approximate criterion that  $|\Delta\rho_a|/|\Delta\rho_c|$  has to be greater than a factor of 5, then  $v/c$  has to be less than 15% or the horizontal phase velocity has to be less than 45 m s<sup>-1</sup>. This covers a fairly large range and includes most of the observed mid-altitude small-scale GW from airglow data.

The vertical dashed line indicates the position where  $k_z^2 =$

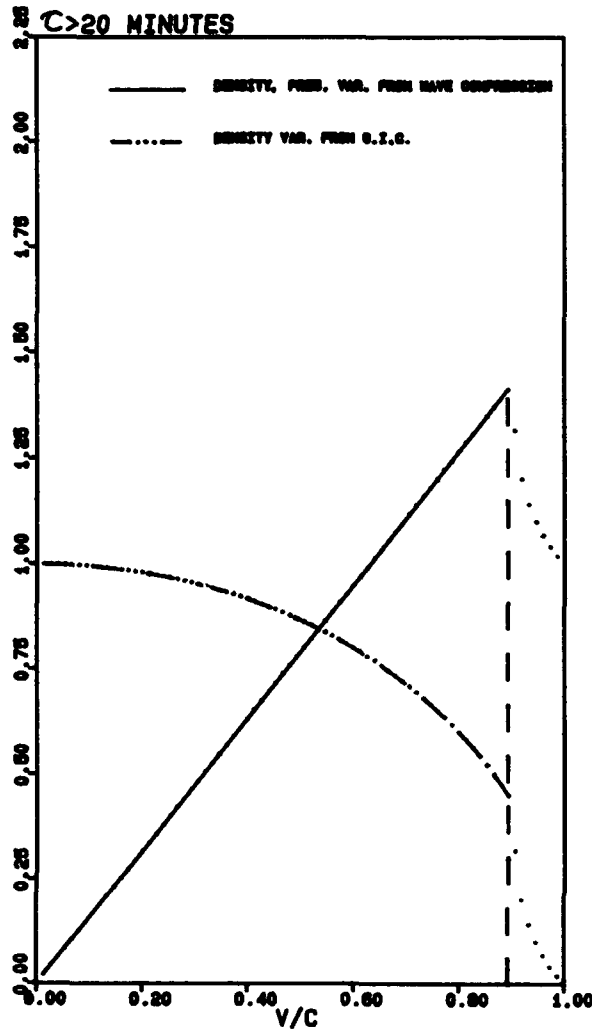


Fig. 1. Plot of the induced density variation due to the gravitational (dash-dot-dot curve) and the acoustic compressions (solid curve) as a function of  $v/c$  for wave periods of  $>20$  min.

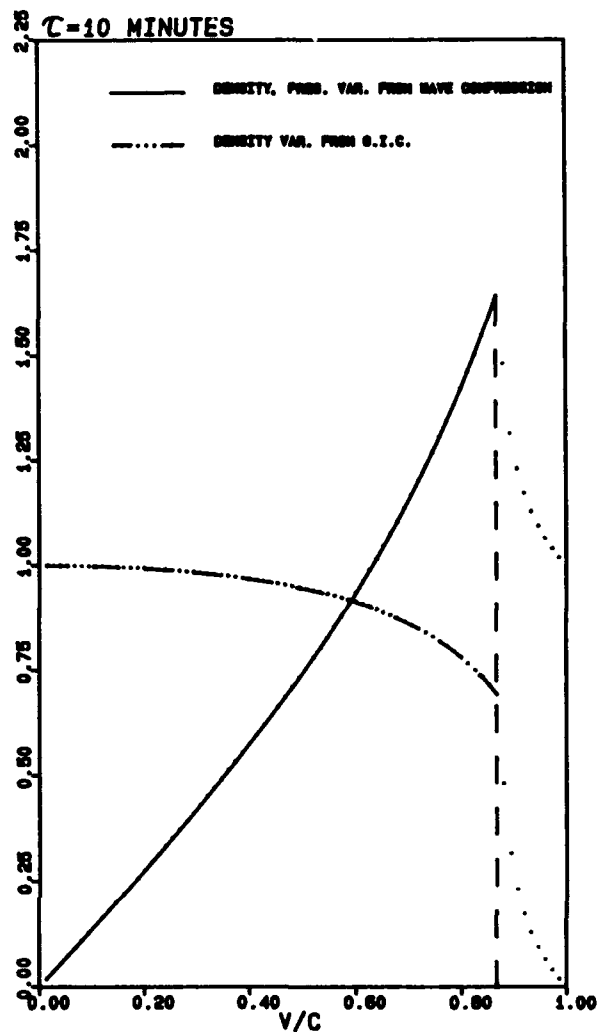


Fig. 2. Plot of the induced density variation due to the gravitational (dash-dot-dot curve) and the acoustic compressions (heavy solid curve) as a function of  $v/c$  for a wave period of 10 min.

0. It is easy to show from Hines' dispersion formula that  $k_z^2 = 0$  corresponds to

$$\frac{v}{c} = \left( \frac{\omega_b^2 - \omega^2}{\omega_a^2 - \omega^2} \right)^{1/2} \quad (7)$$

To the left of the vertical line,  $k_z^2 > 0$ , and GW may propagate freely. To its right,  $k_z^2 < 0$ , and the GW is evanescent in the vertical direction, although it still propagates along  $k_x$ . The dotted lines represent the evanescent region. At  $v/c = 1$  we have the Lamb mode for which there is no GIC compression since there is no vertical motion and variations in density are caused entirely by wave compression, an exact reversal of what happens at  $v/c = 0$ . The same reversal occurs in all the figures.

As  $\tau \rightarrow \tau_b$ , the Brunt period, both  $|\Delta \rho_a|/|\Delta \rho|$  and  $|\Delta \rho_c|/|\Delta \rho|$  increase with  $v/c$  (see Figures 3 and 4) in such a way that the GIC compression continues to predominate over a much greater range of horizontal phase velocity. In fact, in Figure 4 where  $\tau = 5.2$  min, the GIC compression continues to dominate all the way to the dashed line where  $v/c \sim 42\%$ , corresponding to a horizontal phase velocity of well over 120

$\text{m s}^{-1}$ : a strictly medium-scale GW [Francis, 1975]. Thus as the GW period approaches the Brunt period, the GIC compression dominates over a larger range of  $v$  and hence a larger range of wavelengths.

The pressure variation can be easily shown to be the same as  $\Delta \rho_c$ . Using the linearized horizontal momentum conservation equation, it can be shown that for monochromatic waves,

$$\Delta p = v \rho_0 u$$

or

$$\frac{\Delta p}{\rho_0} = \frac{\gamma v u}{c^2}$$

so

$$\frac{|\Delta p|}{c^2 |\Delta \rho|} = \frac{|\Delta \rho_c|}{|\Delta \rho|} \quad (8)$$

From Figures 1–4 we see that there is little pressure variation produced by wave compression for small-scale

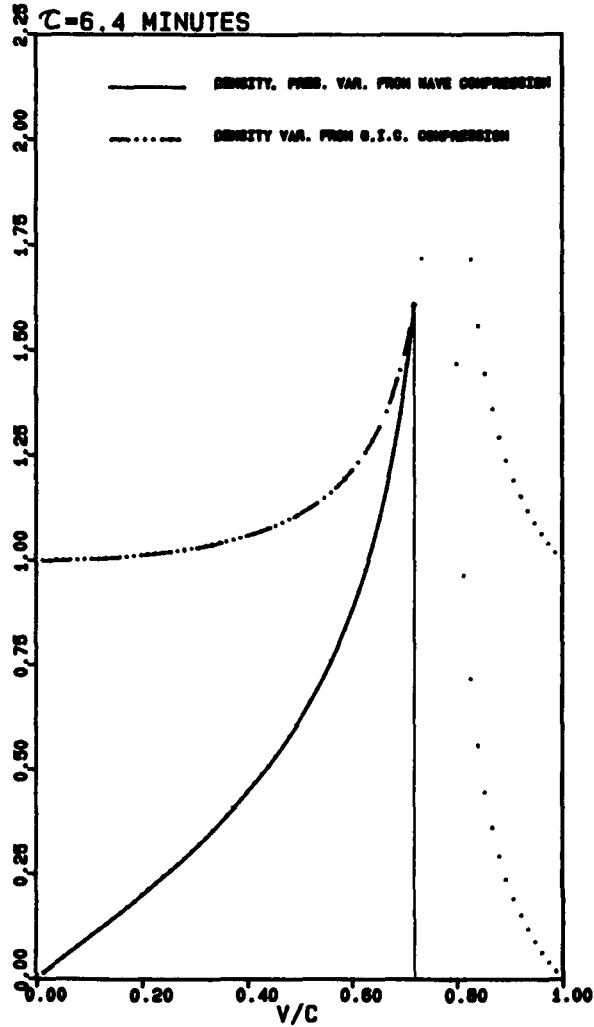


Fig. 3. Same as Figure 2 except for a wave period of 6.4 min.

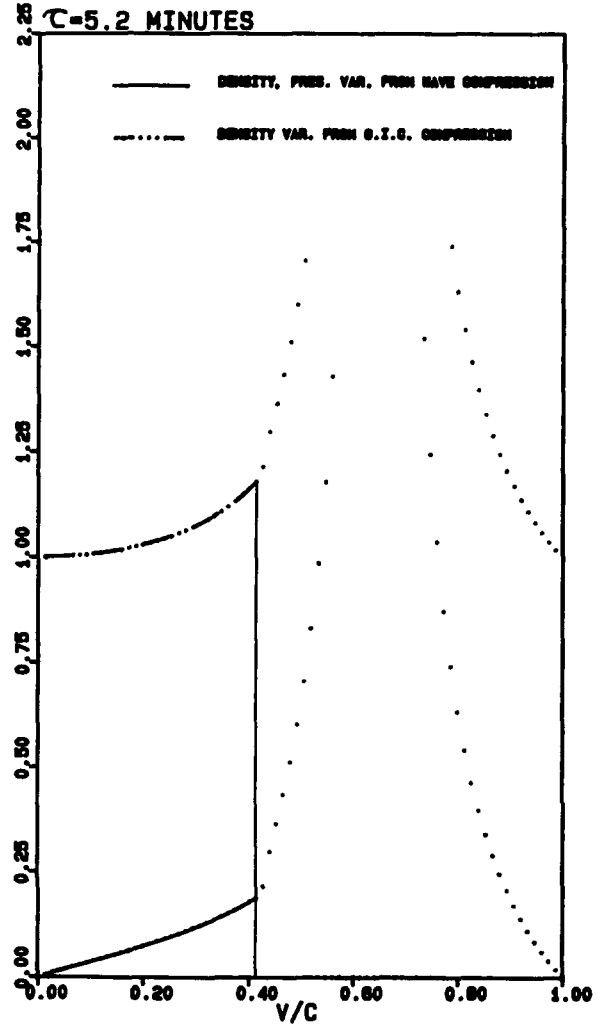


Fig. 4. Same as Figure 2 except for a wave period of 5.2 min.

GW. Only as the scale size of the GW increases does it become important. Thus for small-scale GW ( $<45 \text{ m s}^{-1}$ ) the pressure variations are relatively insignificant.

The temperature variations may be very easily obtained from the linearized perfect gas law given by

$$\frac{\Delta T}{T_0} = \frac{\Delta p}{p_0} - \frac{\Delta \rho}{\rho_0} \quad (9)$$

From (7), (9), and (2a) we obtain

$$\frac{\Delta T}{T_0} = (\gamma - 1) \left( \frac{vu}{c^2} \right) - \frac{\Delta \rho_a}{\rho_0} \quad (10)$$

Thus for  $v \ll c$  (small-scale GW),

$$\frac{\Delta T}{T_0} = -\frac{\Delta \rho_a}{\rho_0} = -\frac{(\gamma - 1)h}{\gamma H} \quad (11)$$

and the temperature variation is opposite in phase to the GIC density compression. We will define

$$\frac{\Delta T}{T_0} = \frac{\Delta T_a}{T_0} + \frac{\Delta T_c}{T_0} \quad (12)$$

where

$$\frac{\Delta T_a}{T_0} = -\frac{\Delta \rho_a}{\rho_0} \quad \frac{\Delta T_c}{T_0} = (\gamma - 1) \frac{vu}{c^2}$$

Again, as in (3) and (4) it is possible to show that for  $k_z^2 > 0$  (see Appendix 3),

$$\frac{|\Delta T_a|}{|\Delta T|} = \left[ \frac{1 - (v/c)^2}{1 - (\gamma - 1)(\omega/\omega_b)^2(v/c)^2} \right]^{1/2} \quad (13)$$

$$\frac{|\Delta T_c|}{|\Delta T|} = \left[ \frac{(\gamma - 1)(1 - (\omega/\omega_b)^2)}{1 - (\gamma - 1)(\omega/\omega_b)^2(v/c)^2} \right]^{1/2} \left( \frac{v}{c} \right) \quad (14)$$

Thus once again, for  $v/c = 0$ ,  $|\Delta T_a|/|\Delta T| = 1$  and  $|\Delta T_c|/|\Delta T| = 0$ , and we see that in the low phase velocity limit (very small scale GW) the temperature variation is caused entirely by the adiabatic expansion and compression of an air parcel oscillating in the vertical direction. For long-period GW ( $\omega \ll \omega_b$ ), (13) and (14) simplify to

$$\frac{|\Delta T_a|}{|\Delta T|} \sim \left[ 1 - \left( \frac{v}{c} \right)^2 \right]^{1/2} \quad (15)$$

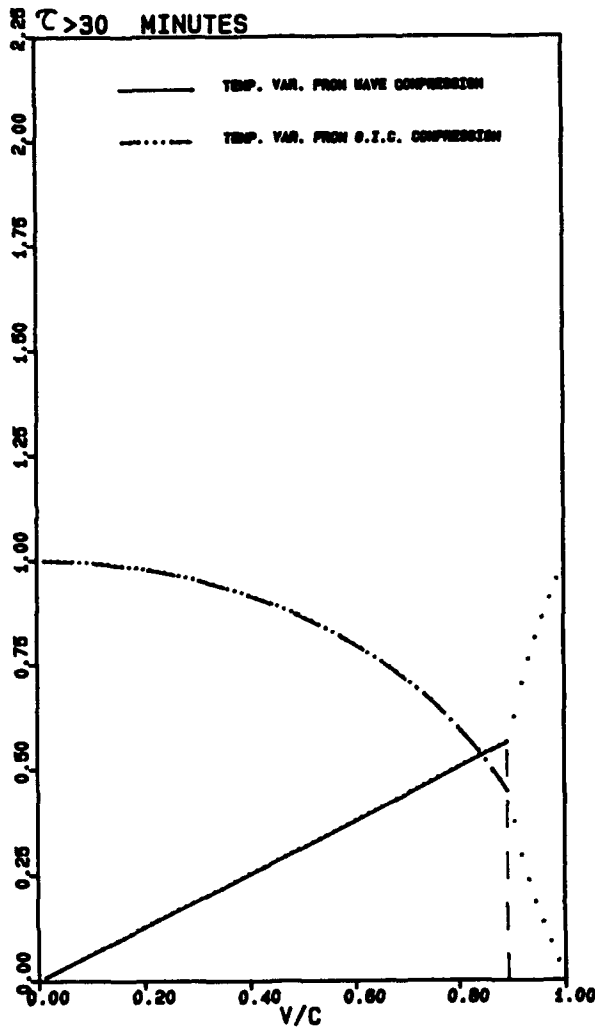


Fig. 5. Plot of the induced temperature variation due to the gravitational (dash-dot-dot curve) and the acoustic compressions (solid curve) as a function of  $v/c$  for wave periods of  $>30$  min.

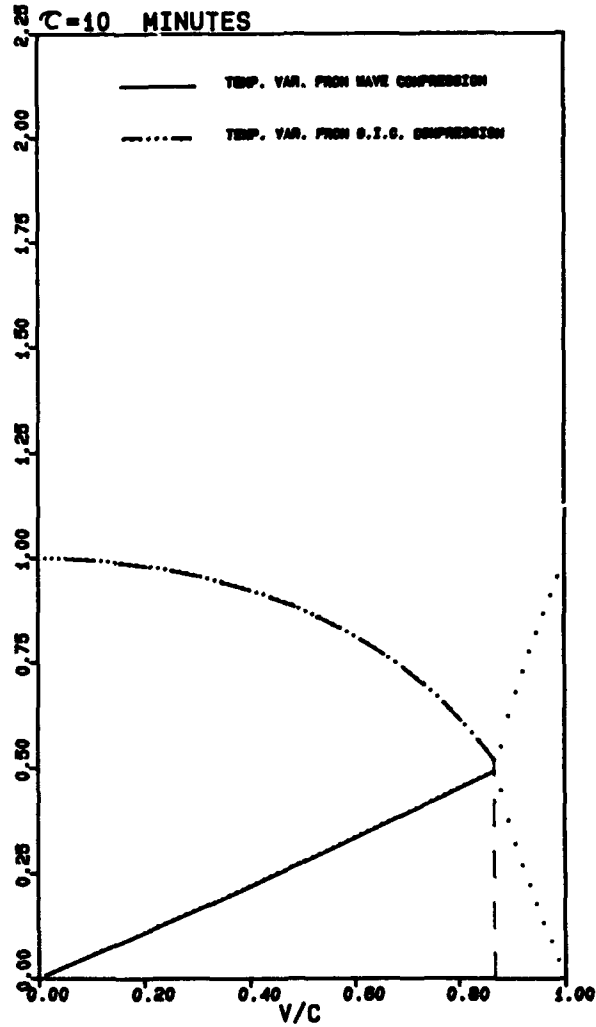


Fig. 6. Plot of the induced temperature variation due to the gravitational (dash-dot-dot curve) and the acoustic compressions (solid curve) as a function of  $v/c$  for a wave period of 10 min.

$$\frac{|\Delta T_c|}{|\Delta T|} \sim (\gamma - 1)^{1/2} \left( \frac{v}{c} \right) \quad (16)$$

Comparing (15) and (16) with (5) and (6), we see that for long-period GW,  $|\Delta T_a|/|\Delta T|$  behaves in the same way as  $|\Delta \rho_a|/|\Delta \rho|$  in (5) while  $|\Delta T_c|/|\Delta T|$  has a far more gradual slope than  $|\Delta \rho_c|/|\Delta \rho|$ . Thus for temperature variations the GIC effect predominates over the "wave effect" through a greater range of phase velocities.

All this can be seen from Figure 5, which shows the behavior of  $|\Delta T_a|/|\Delta T|$  and  $|\Delta T_c|/|\Delta T|$  for GW with periods from 30 min on up. Again, a plot of both curves at  $\tau = 120$  min can be exactly superimposed over the two curves for  $\tau = 30$  min. This is similar to the curve of the density variations (Figure 1) which has a lower limit at  $\tau = 20$  min. Again, for  $\tau > 30$  min there is no significant difference between (13) and (15) or (14) and (16).

Figures 6, 7, and 8 show the behavior of temperature variations for  $\tau = 10, 6.4$ , and  $5.2$  min, respectively. The big difference between these temperature variations and the density variations given by Figures 2, 3, and 4 is that for the former the effect of GIC compression is even much more important than the wave compression. For instance, at  $\tau =$

$6.4$  min the wave compression effect overtakes the GIC effect at  $v/c = 0.72$ , whereas the GIC effect remains predominant in the corresponding temperature variation all the way to the vertical dashed line. For both, however, the GIC effect predominates all the way to the dashed line when  $\tau = 5.2$  min, approaching the Brunt period.

The dotted curves in all the figures on the right-hand side of the dashed line correspond to evanescent waves with  $k_z^2 < 0$  and thus a purely imaginary  $k_z$ . In this region one can no longer use the relatively simple expressions given by (3), (4), (13), and (14), which were derived for  $k_z^2 > 0$  and real  $k_z$ . Instead one has to work with the general polarization relations given by Hines [1960].

From the above discussions, it is clear that comparatively small scale GW with horizontal phase velocities less than  $40\text{--}50 \text{ m s}^{-1}$  may be considered to be purely under the influence of GIC expansion and compression ( $>90\%$ ). This will allow us to make simple conversions from the measurement of temperature fluctuations to height fluctuations. Thus

$$\frac{|\Delta T|}{T_0} \sim \frac{|\Delta T_a|}{T_0} = \frac{(\gamma - 1)}{\gamma} \frac{h}{H} \quad (17)$$

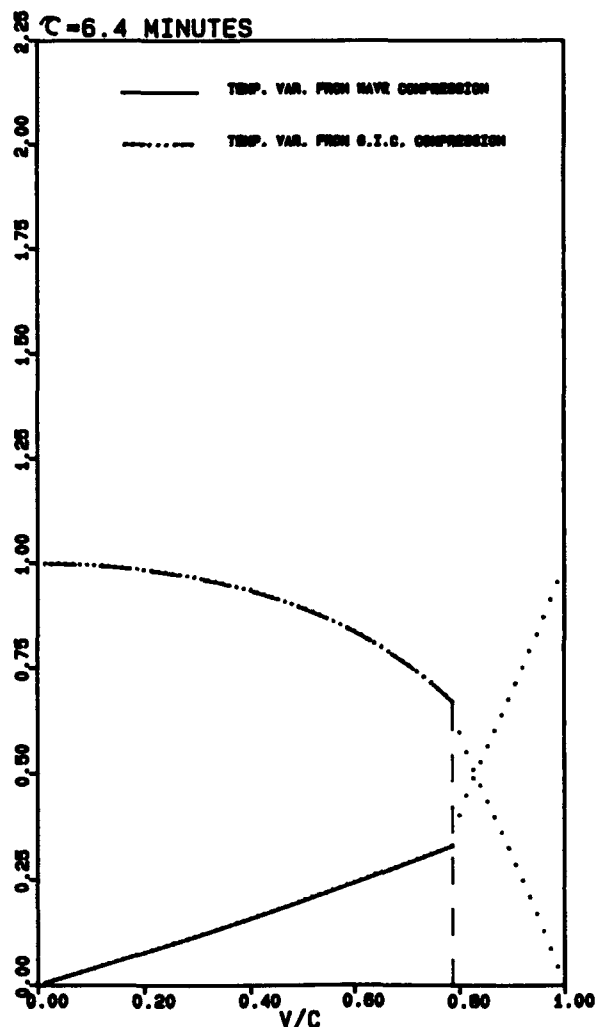


Fig. 7. Same as Figure 6 except for a wave period of 6.4 min.

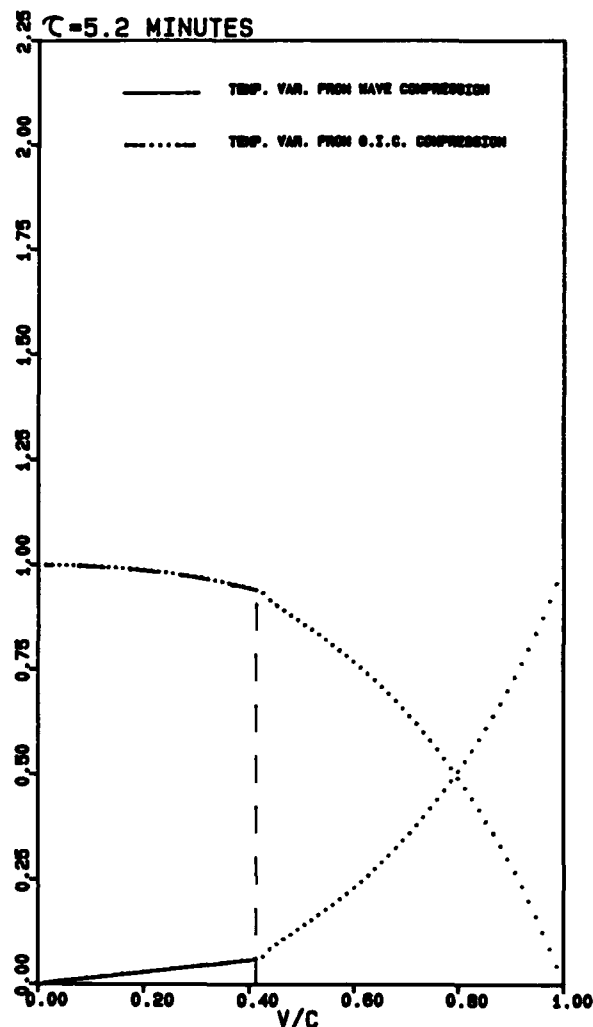


Fig. 8. Same as Figure 6 except for a wave period of 5.2 min.

and using the usual values for  $\gamma$ ,  $H$ , and  $T_0$ , we obtain the approximate conversion that a  $10^\circ$  variation in temperature corresponds approximately to a height variation of 1 km at 90–100 km altitude.

This can be immediately used for computing the time-averaged kinetic energy density, KE, given by

$$KE = \frac{1}{4} \rho_0 (|u|^2 + |w|^2) \quad (18)$$

where  $w$  is the vertical particle velocity. Using the continuity equation and Hines' dispersion relations, one can show that (Appendix 4)

$$KE = \frac{1}{4} \rho_0 \omega_b^2 |h|^2 \left[ \frac{1 - (\omega/\omega_b)^2 (v/c)^2}{1 - (v/c)^2} \right] \quad (19)$$

For large-scale GW where  $v \rightarrow c$ , the denominator can be much less than the numerator. This is especially true for long-period GW. Thus the KE can then be much greater than  $\frac{1}{4} \rho_0 \omega_b^2 |h|^2$ . For small-scale GW ( $v \ll c$ ), on the other hand, the KE is very accurately given by

$$KE = \frac{1}{4} \rho_0 \omega_b^2 |h|^2 \quad (20a)$$

It is interesting to note that (20a) is true irrespective of the frequency of the small-scale GW. Since (20a) is also the KE

for the natural Brunt oscillation of a parcel of air, we may conclude that the total KE of small-scale GW at any frequency is equivalent to natural vertical atmospheric oscillations with the same vertical displacement. Here the GIC approximations for the density, pressure, and temperature variations are also good. Using (17), (20a) acquires the form

$$\begin{aligned} \frac{KE}{p_0} &= \frac{1}{4} \left( \frac{\gamma}{\gamma - 1} \right) \left| \frac{\Delta T_a}{T_0} \right|^2 \sim \frac{1}{4} \left( \frac{\gamma}{\gamma - 1} \right) \left| \frac{\Delta T}{T_0} \right|^2 \\ &= 0.875 \left| \frac{\Delta T}{T_0} \right|^2 \quad (20b) \end{aligned}$$

where  $p_0$  is the background pressure energy. Thus a measurement of the rotational temperature variation can immediately yield the total kinetic energy density at any frequency for small-scale GW. In fact, (19) shows that the KE depends strongly on frequency only for large-scale GW where  $v \rightarrow c$  (see Figure 9).

To summarize: (1) for small-scale GW ( $v < 45$ – $50 \text{ m s}^{-1}$ ) the KE density is the same as that for natural atmospheric oscillations and is independent of wave frequency; (2) for any GW (arbitrary  $v/c$ ) the KE again becomes equal to natural atmospheric oscillations when  $\omega \rightarrow \omega_b$  as expected; and (3) for large-scale GW ( $v/c \rightarrow 1$ ) the KE for the same

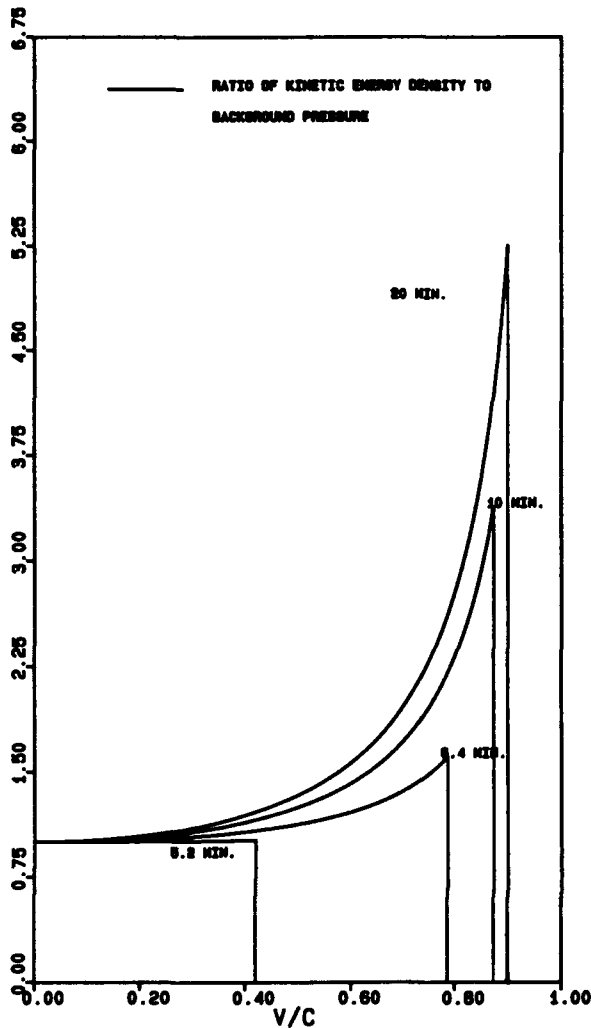


Fig. 9. Plot of the ratio of the kinetic energy density to the background pressure as a function of  $v/c$  for wave periods of 20, 10, 6.4, and 5.2 min.

vertical displacement becomes very large and, unlike the two previous cases, can also become very strongly frequency dependent.

#### 4. APPLICATIONS

To specifically apply the above analyses, we apply them to three specific sets of observed data: two sets involve GW parameters well within the above mentioned limits for the validity of the purely GIC model; the other involves parameters above the borderline. The first set were data taken by *Taylor and Hapgood* [1988]. The observed data include a GW with a horizontal phase velocity of  $v = 21.7 \text{ m s}^{-1}$ , a horizontal wavelength of  $\lambda_x = 26 \text{ km}$ , and a period  $\tau = 20 \text{ min}$ . Using  $g = 9.8 \text{ m s}^{-2}$ ,  $H = 6.56 \text{ km}$ ,  $\gamma = 1.4$ ,  $\tau_b = 5.1 \text{ min}$  (the Brunt period), and the speed of sound  $c = 300 \text{ m s}^{-1}$ , we find that if we employ the full expression given by (10) with help from *Hines*' [1960] polarization and dispersion relations we obtain

$$\frac{|\Delta T|}{T_0} = 4.364 \times 10^{-2} |h| \quad (21)$$

where  $h$  is expressed in kilometers. Using the GIC approximation, we obtain

$$\frac{|\Delta T_a|}{T_0} = \frac{(\gamma - 1)}{\gamma} \frac{|h|}{H} = 4.355 \times 10^{-2} |h| \quad (22)$$

The error from using (22) is only 0.2%.

The second set of data were taken by *Clairemidi et al.* [1985]. They have measured waves with velocity  $v = 15.6 \text{ m s}^{-1}$  and a period of 48 min. The full temperature fluctuation without approximation is given by

$$\frac{|\Delta T|}{T_0} = 4.36 \times 10^{-2} |h| \quad (23)$$

Compared with the GIC approximation given by (22), we have an error of the order of 0.1%.

The third set of data were taken by *Witt* [1962]. The GW had  $v = 75 \text{ m s}^{-1}$  and  $\lambda_x = 50 \text{ km}$ , and the rest of the parameters are the same as the first data set. We obtain

$$\frac{|\Delta T|}{T_0} = 4.5 \times 10^{-2} |h| \quad (24)$$

The GIC approximation gives the same result as (22). Thus the error for this example is 3%. The somewhat bigger error is understandable because at  $75 \text{ m s}^{-1}$  the horizontal phase velocity is somewhat above the  $45\text{--}50 \text{ m s}^{-1}$  upper limit that we mentioned earlier as the safe limit (i.e.,  $v/c \sim 15\text{--}20\%$ ). Actually, for this example there is considerable interference between the two terms on the right-hand side of (10).

#### 5. CONCLUSION

The present paper seems to show that for small-scale GW (say  $v/c < 18\%$ ) the GIC approximation is very good to above 95% in temperature and density fluctuations. The approximation appears to be applicable to many of the observed mid-altitude airglow data. Quick estimates of and simple formulas for GW parameters such as height variations and kinetic energy density may be immediately obtained from measurement of temperature variations.

#### APPENDIX 1

We can derive equation (2a) by using the usual expression for  $\Delta\rho/\rho_0$  [*Hines*, 1960], given by

$$\frac{\Delta\rho}{\rho_0} = \left\{ \omega^2 k_z + i \left[ (\gamma - 1) g k_x^2 - \frac{\gamma g \omega^2}{2c^2} \right] \right\} f \quad (A1)$$

where  $f = \alpha e^{z/2H} e^{i(\omega t - k \cdot r)}$ .

We eliminate  $\omega$  by using  $\omega = k_x v$  and substitute in for the scale height  $H = c^2/\gamma g$  to obtain

$$\frac{\Delta\rho}{\rho_0} = \left\{ k_x^2 k_z v^2 + i k_x^2 c^2 \left[ \left( \frac{\gamma - 1}{\gamma} \right) \frac{1}{H} - \frac{v^2}{2Hc^2} \right] \right\} f \quad (A2)$$

We obtain, by adding and subtracting  $(v/c)^2(\gamma - 1/\gamma H)$  in (A2),

$$\frac{\Delta\rho}{\rho_0} = \left\{ k_x^2 k_z v^2 + i k_x^2 c^2 \left[ \left( 1 - \left( \frac{v}{c} \right)^2 \right) \left( \frac{\gamma - 1}{\gamma H} \right) - \frac{v^2}{Hc^2} \left( \frac{1}{\gamma} - \frac{1}{2} \right) \right] \right\} f \quad (A3)$$

Introducing the vertical displacement field,

$$\frac{h}{H} = \frac{w}{i\omega H} = ik_x^2 c^2 \left( \frac{1}{H} \right) \left[ 1 - \left( \frac{v}{c} \right)^2 \right] f \quad (\text{A4})$$

we get

$$\frac{\Delta \rho}{\rho_0} = \left( \frac{\gamma - 1}{\gamma} \right) \frac{h}{H} + k_x^2 v^2 \left[ k_z - i \left( 1 - \frac{\gamma}{2} \right) \frac{g}{c^2} \right] f \quad (\text{A5})$$

Finally, we use

$$u = k_x^2 c^2 v [k_z - i(1 - \gamma/2)g/c^2]f$$

to obtain

$$\frac{\Delta \rho}{\rho_0} = \left( \frac{\gamma - 1}{\gamma} \right) \frac{h}{H} + \frac{uv}{c^2} \quad (\text{A6})$$

which is exactly equation (2a).

## APPENDIX 2

From now on we consider only  $k_z^2 > 0$  (i.e.,  $k_z$  real). To obtain equation (3), we note (using (A4)) that

$$\begin{aligned} \frac{|\Delta \rho_a|}{\rho_0} &= \left( \frac{\gamma - 1}{\gamma} \right) \frac{|h|}{H} = (\gamma - 1) k_x^2 g \left[ 1 - \left( \frac{v}{c} \right)^2 \right] |f| \\ &= \left( \frac{\gamma - 1}{\gamma} \right) \left( \frac{1}{H} \right) \left( \frac{c^2}{v^2} - 1 \right) \omega^2 |f| \quad (\text{A7}) \end{aligned}$$

Using (A1), eliminating  $k_x$  and  $g$ , and substituting in  $\eta = -(1 - \gamma/2)g/c^2$ , we obtain

$$\frac{|\Delta \rho|}{\rho_0} = \left\{ k_z^2 + \left[ \left( \frac{\gamma - 1}{\gamma} \right) \frac{1}{H} \left( \frac{c^2}{v^2} - 1 \right) + \eta \right]^2 \right\}^{1/2} \omega^2 |f| \quad (\text{A8})$$

Using the dispersion relation [Hines, 1960] and letting  $\varepsilon = c^2/v^2 - 1$ , we have

$$k_z^2 = \frac{\omega_b^2 - \omega^2}{v^2} - \frac{\omega_a^2 - \omega^2}{c^2} = \frac{\omega_b^2 - \omega^2}{c^2} \varepsilon - |\eta|^2 \quad (\text{A9})$$

where  $\eta^2 = (\omega_a^2 - \omega_b^2)/c^2$ . Thus

$$\begin{aligned} \frac{|\Delta \rho_a|}{|\Delta \rho|} &= \left( \frac{\gamma - 1}{\gamma} \right) \frac{\varepsilon}{H} \\ &\cdot \left\{ \frac{\omega_b^2 - \omega^2}{c^2} \varepsilon + \left[ \left( \frac{\gamma - 1}{\gamma} \right) \frac{1}{H} \right]^2 \varepsilon^2 \right. \\ &+ \varepsilon \frac{2(\gamma - 1)\eta}{\gamma H} \left. \right\}^{-1/2} = \left\{ \left( \frac{\gamma - 1}{\gamma} \right)^2 \frac{\varepsilon}{H^2} \right. \\ &\cdot \left[ \frac{\omega_b^2 - \omega^2}{c^2} + \left( \left( \frac{\gamma - 1}{\gamma} \right) \frac{1}{H} \right)^2 \varepsilon \right. \\ &\left. \left. - \left( \frac{\gamma - 1}{\gamma} \right) \frac{(2 - \gamma)g}{Hc^2} \right]^{-1} \right\}^{1/2} \quad (\text{A10}) \end{aligned}$$

Using  $\omega_b^2 = (\gamma - 1)g^2/c^2$  and dividing it from the numerator and the denominator, we obtain

$$\frac{|\Delta \rho_a|}{|\Delta \rho|} = \left[ \frac{(\gamma - 1)\varepsilon}{1 - (\omega/\omega_b)^2 + (\gamma - 1)\varepsilon + (\gamma - 2)} \right]^{1/2}$$

so

$$\frac{|\Delta \rho_a|}{|\Delta \rho|} = \left[ \frac{(\gamma - 1)(1 - (v/c)^2)}{(\gamma - 1) - (\omega/\omega_b)^2(v/c)^2} \right]^{1/2} \quad (\text{A11})$$

which is equation (3).

To compute  $|\Delta \rho_c|/|\Delta \rho|$ , we note that

$$\frac{\Delta \rho_c}{\rho_0} = \frac{uv}{c^2} = \frac{v}{c^2} \left\{ \omega k_x^2 c^2 \left[ k_z - i \left( 1 - \frac{\gamma}{2} \right) \frac{g}{c^2} \right] \right\} f \quad (\text{A12})$$

where, again, we use the polarization relation for  $u$  [Hines, 1960]. Substituting for  $\eta$ ,

$$\Delta \rho_c / \rho_0 = v/c^2 [\omega k_x^2 c^2 (k_z + i\eta)] f \quad (\text{A13})$$

so

$$\frac{|\Delta \rho_c|}{|\Delta \rho|} = \left\{ \frac{k_z^2 + \eta^2}{k_z^2 + [((\gamma - 1)/\gamma)(1/H)\varepsilon + \eta]^2} \right\}^{1/2} \quad (\text{A14})$$

where we have used (A8) and (A13). Using (A9), we obtain

$$\begin{aligned} \frac{|\Delta \rho_c|}{|\Delta \rho|} &= \left\{ \frac{\omega_b^2 - \omega^2}{c^2} \varepsilon \left[ \left( \frac{\omega_b^2 - \omega^2}{c^2} \varepsilon - \eta^2 \right) \right. \right. \\ &+ \left. \left( \frac{\gamma - 1}{\gamma} \frac{\varepsilon}{H} + \eta \right)^2 \right]^{-1} \right\}^{1/2} = \{ (\omega_b^2 - \omega^2)/c^2 [(\omega_b^2 - \omega^2)/c^2 \\ &+ [((\gamma - 1)/\gamma)(1/H)]^2 \varepsilon + 2(\gamma - 1)\eta/\gamma H]^{-1} \}^{1/2} \end{aligned}$$

so

$$\frac{|\Delta \rho_c|}{|\Delta \rho|} = \left\{ \frac{1 - (\omega/\omega_b)^2}{(\gamma - 1) - (\omega/\omega_b)^2(v/c)^2} \right\}^{1/2} (v/c) \quad (\text{A15})$$

which is equation (4).

## APPENDIX 3

From (10) we write

$$\begin{aligned} \frac{\Delta T}{T_0} &= (\gamma - 1) \frac{vu}{c^2} - \frac{(\gamma - 1)h}{\gamma H} = (\gamma - 1) \{ v/c^2 [\omega k_x^2 c^2 (k_z + i\eta)] \\ &- ik_x^2 g(v/c)^2 (c^2/v^2 - 1) \} f \quad (\text{A16}) \end{aligned}$$

where we have used (A4) and (A13). Thus

$$\Delta T/T_0 = (\gamma - 1)k_x^2 v^2 \{ k_z + i[\eta - g/c^2(c^2/v^2 - 1)] \} f$$

and since  $\Delta T_a/T_0 = -\Delta \rho_a/\rho_0$  (see (12)), we obtain by using (A7)

$$\frac{|\Delta T_a|}{|\Delta T|} = \frac{(\gamma - 1)(k_x^2 v^2 g/c^2) \varepsilon}{(\gamma - 1)k_x^2 v^2 [k_z^2 + (\eta - (g/c^2)\varepsilon)^2]^{1/2}} \quad (\text{A17})$$

Using again the dispersion relation for  $k_z^2$ , we obtain



$$\frac{|\Delta T_a|}{|\Delta T|} = (g/c^2) \varepsilon \left[ \frac{\omega_b^2 - \omega^2}{c^2} \varepsilon - \frac{2\eta g}{c^2} \varepsilon + \frac{g^2}{c^4} \varepsilon^2 \right]^{-1/2}$$

$$= \frac{\varepsilon^{1/2}}{[1 - (\omega^2 c^2)/g^2 + \varepsilon]^{1/2}} = \left\{ \frac{1 - (v/c)^2}{1 - (\omega^2 v^2)/g^2} \right\}^{1/2}$$

so

$$\frac{|\Delta T_a|}{|\Delta T|} = \left\{ \frac{1 - (v/c)^2}{1 - (\gamma - 1)(\omega/\omega_b)^2(v/c)^2} \right\}^{1/2} \quad (\text{A18})$$

which is equation (13).

Equation (14) may be similarly obtained. The denominator is the same as (13), as expected, but the numerator is given by  $|(\gamma - 1)uv/c^2|$ , which is identical to (4) except for the additional  $(\gamma - 1)$  factor.

#### APPENDIX 4

The KE density is given by

$$\text{KE} = \frac{1}{4} \rho_0 (|u|^2 + |w|^2) \quad (\text{A19})$$

From the work by Hines [1960] and the definition of  $\eta$ , we may write

$$u = \omega k_x c^2 [k_z + i\eta] f \quad (\text{A20})$$

$$w = -\omega k_x^2 c^2 [1 - (v/c)^2] f \quad (\text{A21})$$

so

$$|u|^2 = \frac{k_z^2 + \eta^2}{k_x^2 [1 - (v/c)^2]^2} |w|^2$$

From the dispersion relation

$$\left( \frac{k_z}{k_x} \right)^2 = \frac{\omega_b^2 - \omega^2}{\omega^2} - \left( \frac{v}{c} \right)^2 \frac{\omega_a^2 - \omega^2}{\omega^2}$$

$$\frac{|\eta|^2}{k_x^2} = \left( \frac{v}{c} \right)^2 \frac{\omega_a^2 - \omega_b^2}{\omega^2}$$

Hence

$$|u|^2 + |w|^2 = |w|^2 \left\{ 1 + \frac{[(\omega_b^2/\omega^2) - 1][1 - (v/c)^2]}{(1 - (v/c)^2)^2} \right\} \quad (\text{A22})$$

The total KE then becomes

$$\text{KE} = \frac{1}{4} \rho_0 \omega_b^2 |h|^2 \frac{[1 - (\omega/\omega_b)^2(v/c)^2]}{[1 - (v/c)^2]} \quad (\text{A23})$$

Obviously, (A23) is equation (19).

**Acknowledgments.** We would like to thank R. Picard and J. Winick for helpful discussions. One of us (T.F.T.) would like to thank the National Science Council of the Republic of China for sponsoring his visit to the Atmospheric Physics Department of the National Central University of Chungli, Taiwan, where some of the work was done while the author was on sabbatical leave and where some helpful suggestions were made by several members of the department. The work was sponsored by AFOSR under the MAP-STAR and the Infrared Airglow modeling program. It is partially supported by a research contract with AFGL (AF19628-87K-0026).

The Editor thanks D. Tarasick and another referee for their assistance in evaluating this paper.

#### REFERENCES

- Clairemidi, J., M. Hersh, and G. Moreels, Bi-dimensional observation of waves near the mesopause at auroral latitudes, *Planet. Space Sci.*, **33**, 1013-1022, 1985.
- Dewan, E., T. F. Tuan, and U. Makhlof, On hydrostatic and nonhydrostatic changes of pressure caused by atmospheric gravity waves (abstract), *EOS Trans. AGU*, **69**, 1342, 1988.
- Francis, S. H., Global propagation of atmospheric gravity waves: A review, *J. Atmos. Terr. Phys.*, **37**, 1011-1054, 1975.
- Fritts, D., Gravity wave saturation in the middle atmosphere: A review of theory and observation, *Rev. Geophys.*, **22**, 275-308, 1984.
- Hines, C. O., Internal atmospheric gravity waves at ionospheric heights, *Can. J. Phys.*, **38**, 1441-1481, 1960.
- Lindzen, R. S., Turbulence and stress owing to gravity wave and tidal breakdown, *J. Geophys. Res.*, **86**, 9707-9714, 1981.
- Taylor, M. J., and M. A. Hapgood, Identification of a thunderstorm as a source of short-period gravity waves in the upper atmospheric nightglow emission, *Planet. Space Sci.*, **36**, 975-985, 1988.
- Vincent, R. A., and I. M. Reid, HF Doppler measurements of mesospheric gravity wave momentum fluxes, *J. Atmos. Sci.*, **40**, 1321-1333, 1983.
- Witt, G., Height structure and displacements of noctilucent clouds, *Tellus*, **14**, 1-18, 1962.
- E. Dewan, Optical Physics Division, Air Force Geophysics Laboratory, Hanscom Air Force Base, Bedford, MA 01731.
- J. Isler, U. Makhlof, and T. F. Tuan, Physics Department, University of Cincinnati, Cincinnati, OH 45221.

(Received April 24, 1989;  
revised July 24, 1989;  
accepted August 28, 1989.)

Accession For	
NTIS GRA&I	<input checked="" type="checkbox"/>
DTIC TAB	<input type="checkbox"/>
Unannounced	<input type="checkbox"/>
Justification	
By	
Distribution/	
Availability Codes	
Dist	Avail and/or Special
A-1	20

Unclassified

SECURITY CLASSIFICATION OF THIS PAGE

REPORT DOCUMENTATION PAGE				Form Approved OMB No. 0704-0188	
1a. REPORT SECURITY CLASSIFICATION <b>Unclassified</b>			1b. RESTRICTIVE MARKINGS		
2a. SECURITY CLASSIFICATION AUTHORITY			3. DISTRIBUTION/AVAILABILITY OF REPORT Approved for public release; Distribution unlimited		
2b. DECLASSIFICATION/DOWNGRADING SCHEDULE					
4. PERFORMING ORGANIZATION REPORT NUMBER(S) GL-TR-90-0335			5. MONITORING ORGANIZATION REPORT NUMBER(S)		
6a. NAME OF PERFORMING ORGANIZATION Geophysics Laboratory		6b. OFFICE SYMBOL (if applicable) OPE	7a. NAME OF MONITORING ORGANIZATION		
6c. ADDRESS (City, State, and ZIP Code) Hanscom AFB Massachusetts 01731-5000			7b. ADDRESS (City, State, and ZIP Code)		
8a. NAME OF FUNDING/SPONSORING ORGANIZATION		8b. OFFICE SYMBOL (if applicable)	9. PROCUREMENT INSTRUMENT IDENTIFICATION NUMBER		
8c. ADDRESS (City, State, and ZIP Code)			10. SOURCE OF FUNDING NUMBERS		
PROGRAM ELEMENT NO 61102F		PROJECT NO 2310	TASK NO G2	WORK UNIT ACCESSION NO 01	
11. TITLE (Include Security Classification) On the Importance of the Purely Gravitationally Induced Density, Pressure, and Temperature Variations in Gravity Waves: Their Application to Airglow Observations					
12. PERSONAL AUTHOR(S) U. Makhlouf*, E. Dewan, J.R. Isler*, T.F. Tuan*					
13a. TYPE OF REPORT Reprint		13b. TIME COVERED FROM _____ TO _____		14. DATE OF REPORT (Year, Month, Day) 1990 December 18	
15. PAGE COUNT 9					
16. SUPPLEMENTARY NOTATION *Physics Department, University of Cincinnati, Cincinnati, Ohio - Reprinted from Journal of Geophysical Research, Vol. 95, No. A4, Pages 4103-4111 April 1, 1990					
17. COSATI CODES			18. SUBJECT TERMS (Continue on reverse if necessary and identify by block number)		
FIELD	GROUP	SUB-GROUP	Gravity waves, Airglow, Gravity wavedriven airglow, Compression by gravity waves		
19. ABSTRACT (Continue on reverse if necessary and identify by block number)					
<p>A quantitative study is made of the relative importance of the purely gravitationally induced compression (GIC) due to fluid particle altitude change and the actual "wave compression" which can occur at a fixed altitude in a gravity wave. The results for density, pressure, and temperature variations show the following: (1) the GIC effects predominate (&gt;95%) for <math>v/c &lt; 20\%</math>, where <math>v</math> is the horizontal phase velocity and where very simple formulas can be obtained; (2) the relative importance depends strongly on frequency for wave periods less than 10 min but becomes totally independent of frequency for periods greater than 20 min; and (3) the temperature measurements can be quickly converted to height variations wherever the GIC effect predominates; in general, the conversion is equivalent to the adiabatic lapse rate, i.e., a <math>10^\circ</math> temperature variation corresponds to a height change of 1 km. In addition, the total kinetic energy density can be simply expressed in terms of height variation and, whenever the GIC effects predominate, can be very easily obtained from temperature measurements. An interesting by-product has been that for waves of small horizontal phase speed, the total wave kinetic energy at any frequency is equal to the kinetic energy of the natural (Brunt) oscillation of an air parcel with the same vertical displacement.</p>					
20. DISTRIBUTION/AVAILABILITY OF ABSTRACT <input type="checkbox"/> UNCLASSIFIED/UNLIMITED <input checked="" type="checkbox"/> SAME AS RPT. <input type="checkbox"/> DTIC USERS			21. ABSTRACT SECURITY CLASSIFICATION Unclassified		
22a. NAME OF RESPONSIBLE INDIVIDUAL E. Dewan			22b. TELEPHONE (Include Area Code) (617) 377-4401		22c. OFFICE SYMBOL OPE